Electronic Supplementary Material (ESI) for Journal of Materials Chemistry A.
This journal is © The Royal Society of Chemistry 2021

Supporting Information

Induced crystallization of sol-gel-derived zinc oxide for efficient non-fullerene polymer solar cells

Jiaxin Zheng, Yinqi Luo, Xinbo Wen, Qinglei Zhang, Yu Song, Jiadong Zhou, Nianqiang Jiang, Linlin Liu, Fei Huang, Zengqi Xie *

State Key Laboratory of Luminescent Materials and Devices, Institute of Polymer Optoelectronic Materials and Devices, Guangdong Provincial Key Laboratory of Luminescence from Molecular Aggregates, South China University of Technology, South China University of Technology, Guangzhou 510640, P. R. China. E-mail: msxiez@scut.edu.cn

Table of contents

1. Experimental section.....S3

2. High-resolution transmission electron microscope images.....S6

3. Structural and optoelectronic properties of ZnO films.....S17

4. Water contact angle images.....S19

5. Device performance.....S20

6. References.....S21

1. Experimental section

1.1 Materials

PM6 and Y6 were purchased from Solarmer Material Inc. The other materials and solvents were from common commercial suppliers and used as received. ITO glass with a square resistance of 15 Ω was purchased from South China Science and Technology Co., Ltd.

1.2 Device fabrication and characterization

The ITO glass substrates were cleaned sequentially under sonication with detergent, deionized water, acetone, and isopropyl alcohol, then dried at 80 °C in a baking oven before use. ZnO nanoparticles were prepared according to literatures.[1-2] Zinc acetate dihydrate (2.95 g, 13.4 mmol) was dissolved in methanol (125 ml) with stirring at 60 °C. A solution of KOH (1.48 g, 23 mmol) in methanol (65 ml) was then added dropwise in 15 min. The reaction mixture was stirred for 2.5 h at 60 °C. After cooling to room temperature, the supernatant was removed and the precipitate was washed twice with methanol. Chloroform and 2-methoxyethanol mixture (30 ml, at a volume ratio of 1:1) were added to disperse the precipitate to give a ZnO nanoparticles solution. The solution concentration was about 16 mg/ml. The ZnO precursor solution was prepared by dissolving 1.0 g of zinc acetate dihydrate and 274 ul of ethanolamine in 10 ml of 2-methoxyethanol under vigorous stirring and heating. Blend solution was derived by mixing corresponding volume ratio of ZnO nanoparticles solution and ZnO

precursor solution, then was stirred at 50 °C for 3 h. The optimized volume ratio used in the text was 3:7.

A cathode modification interlayer was prepared by spin-coating the above solution at 3000 rpm for 40 s on the ITO substrate, followed by thermal treatment for 200 °C/1 h. The thicknesses of three different ZnO layers were all approximately 30 nm. The active layer blend PM6:Y6 was dissolved in chloroform (D:A = 1:1.2, 16 mg mL^{-1} in total) with the solvent additive of 1-chloronaphthalene (0.8%, v/v) and spin-casted onto the ZnO layer, then dried at 110 °C for 10 min. The optimal thickness of the photoactive layer was approximately 105 nm. A 10 nm MoO_3 layer and a 100 nm Al layer were subsequently evaporated through a shadow mask to define the active area of the devices (5 mm^2) and form the top anode. Except for the fabrication of ZnO layer, the other processes were all carried out in a nitrogen-filled glovebox.

The current density-voltage (J-V) characteristics were measured using a Keithley 2400 source meter under 1 sun, AM 1.5G spectrum from a solar simulator. The solar simulator illumination intensity was determined using a monocrystal silicon reference cell calibrated by the Konica Minolta Inc. Method of measurement follows JIS C8904-2. The external quantum efficiency (EQE) test was operated by Enlitech QE-R.

1.3 Instruments and measurements

The high-resolution transmission electron microscope (HRTEM) images were taken on JEOL JEM-2100F ZrO/W(100) at 200 kV. The scanning electron microscope (SEM) images were obtained through Hitachi Regulus8100 at 5 kV. Atomic force

microscopy (AFM) images were received through the Bruker Multimode 8 to assess surface appearance of films. The grazing incidence X-ray diffraction (GIXRD) analysis was characterized at a Rigaku SmartLab SE X-ray diffraction system. The work function of samples and the position of the maximum value of valence bands were ascertained by ultraviolet photoelectron spectroscopy (UPS) on ESCALAB 250. Excitation was performed using a He discharge lamp capable of emitting ultraviolet energy at 21.22 eV. The entire UPS measurement was done using standard program with a -5 V bias applied between the sample and the detector. Here, pure gold played a role in reference. The value of work function was calculated by formula ($WF = 21.22 - E_{cutoff}$).

The transient photovoltage (TPV) and transient photocurrent (TPC) were measured by applying 550 nm laser pulses with a power of 2.0 mW. A Nd:YAG laser (Opolette 355 LD, with a repetition rate of 20 Hz and a pulse width of 7 ns) was used as the pump source. The white light bias was triggered by a light-emitting diode. Photovoltage produced a transient voltage signal on a 1 MΩ resistor and photocurrent produced a transient voltage signal on a 50 Ω resistor, which were recorded by a digital oscilloscope.

2. High-resolution transmission electron microscope images

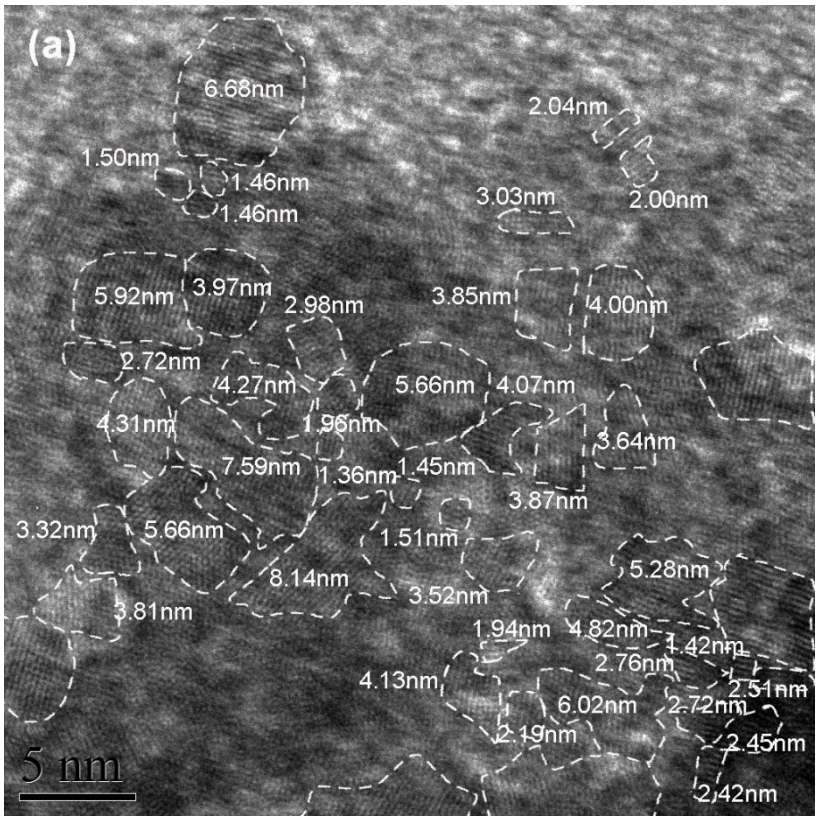

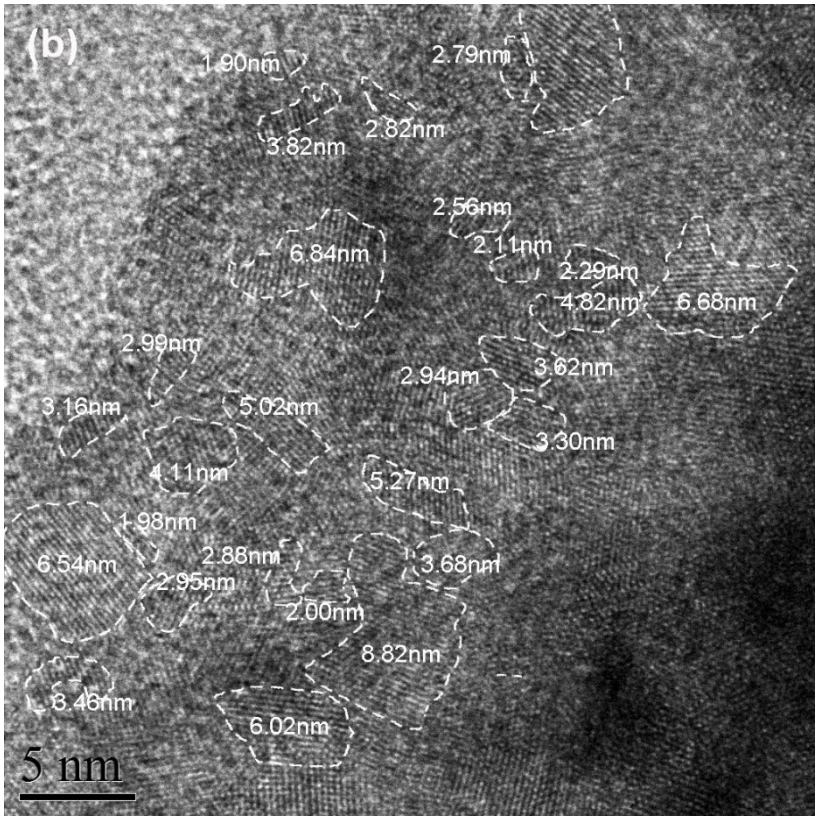

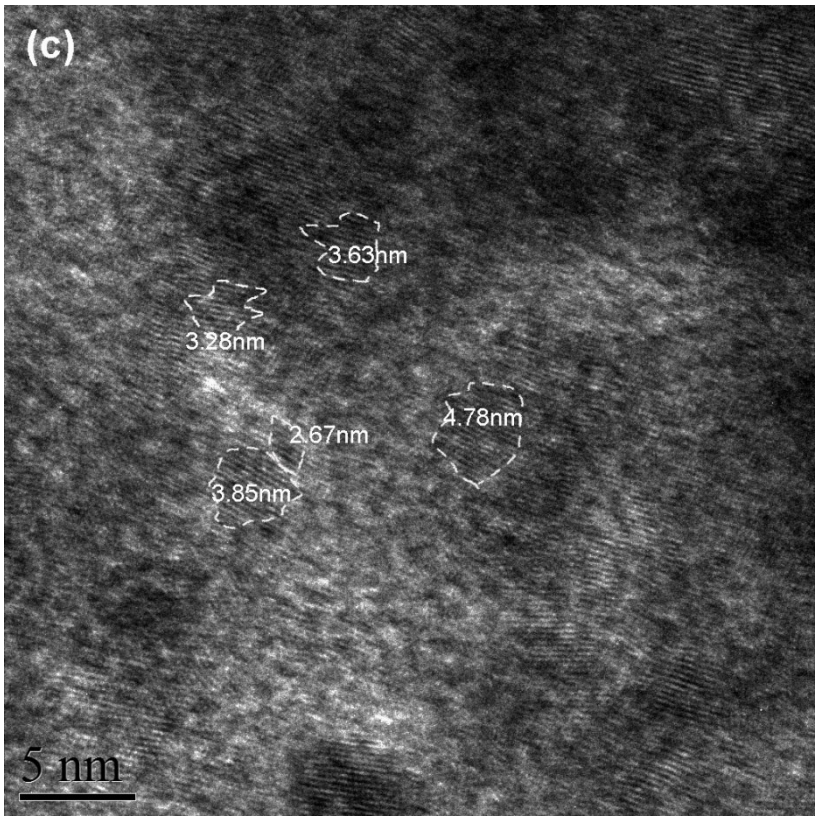
(c)
3.63nm
3.28nm
4.78nm
2.67nm
3.85nm
5 nm

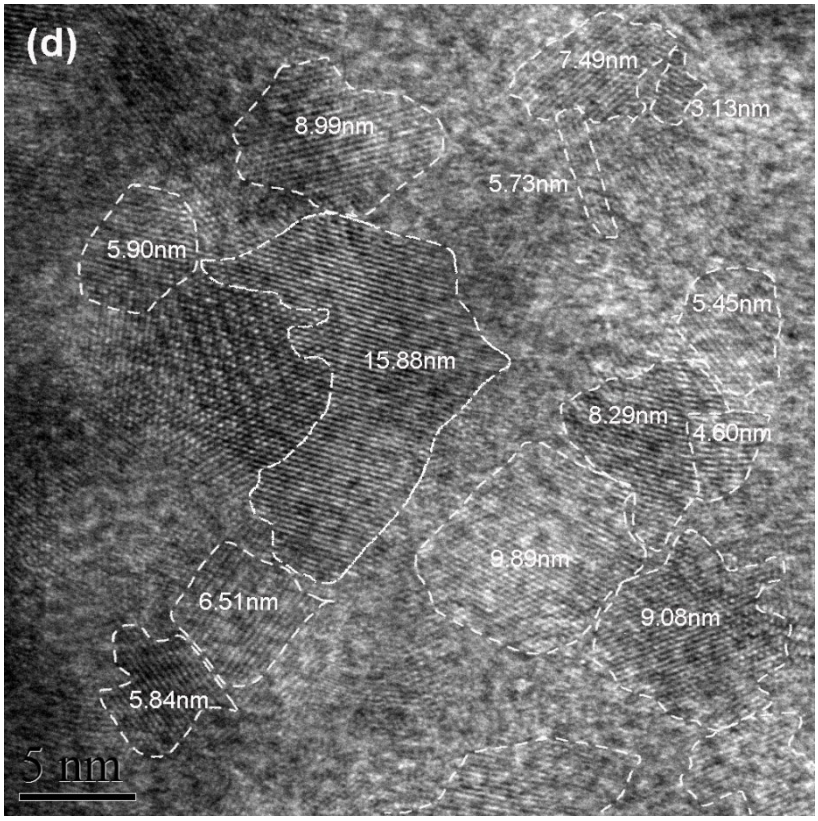
(d)
7.49nm
3.13nm
8.99nm
5.73nm
5.90nm
5.45nm
15.88nm
8.29nm
4.60nm
9.89nm
6.51nm
9.08nm
5.84nm
5 nm

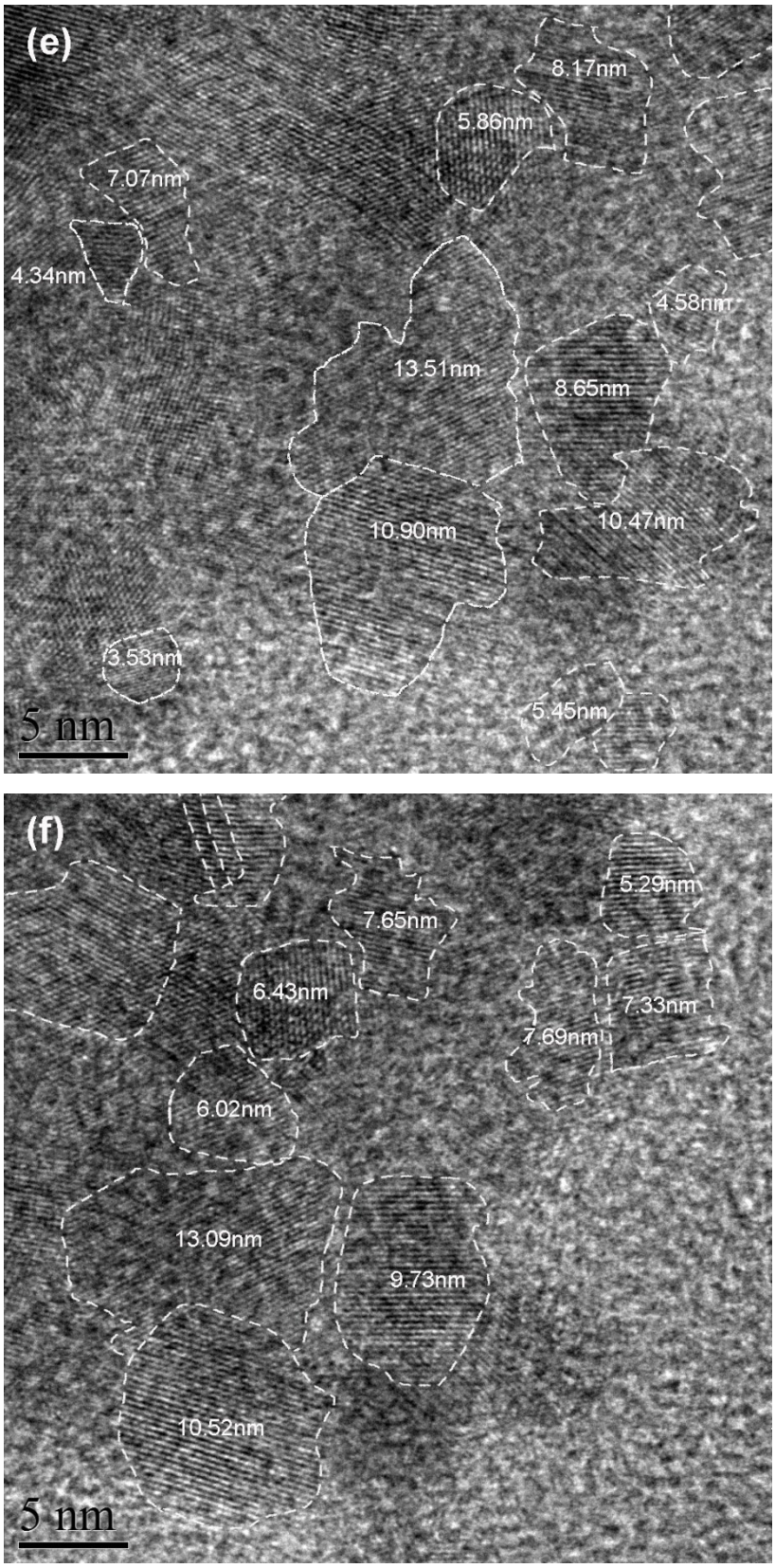
(e)
8.17nm
5.86nm
7.07nm
4.34nm
4.58nm
13.51nm
8.65nm
10.90nm
10.47nm
3.53nm
5.45nm
5 nm
(f)
5.29nm
7.65nm
6.43nm
7.33nm
7.69nm
6.02nm
13.09nm
9.73nm
10.52nm
5 nm

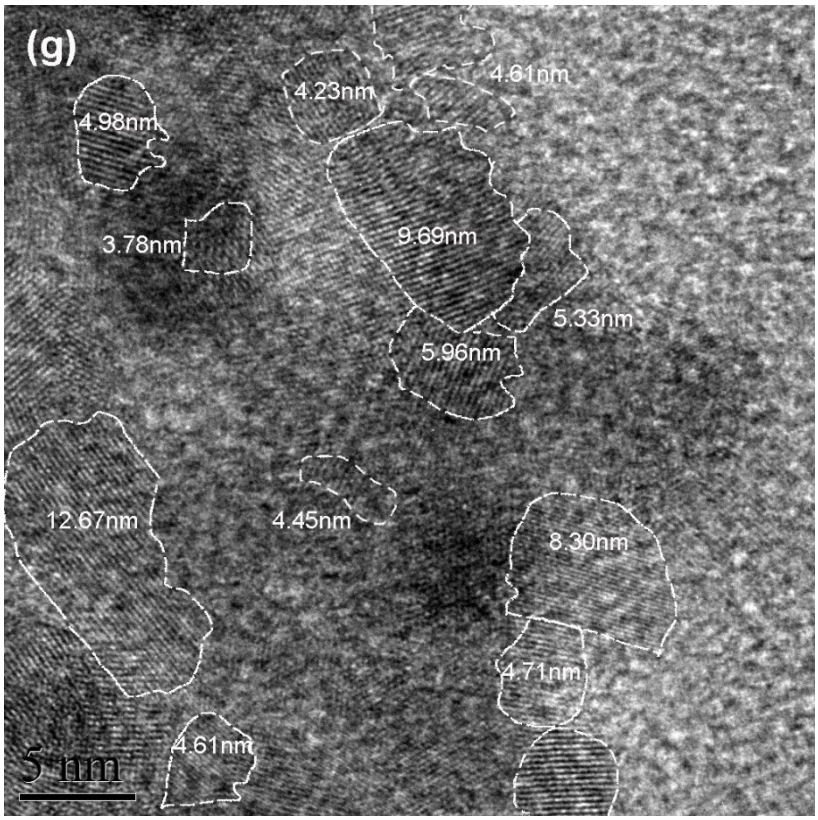
(g)
4.98nm
4.23nm
4.61nm
3.78nm
9.69nm
5.33nm
5.96nm
12.67nm
4.45nm
8.30nm
4.71nm
4.61nm
5 nm

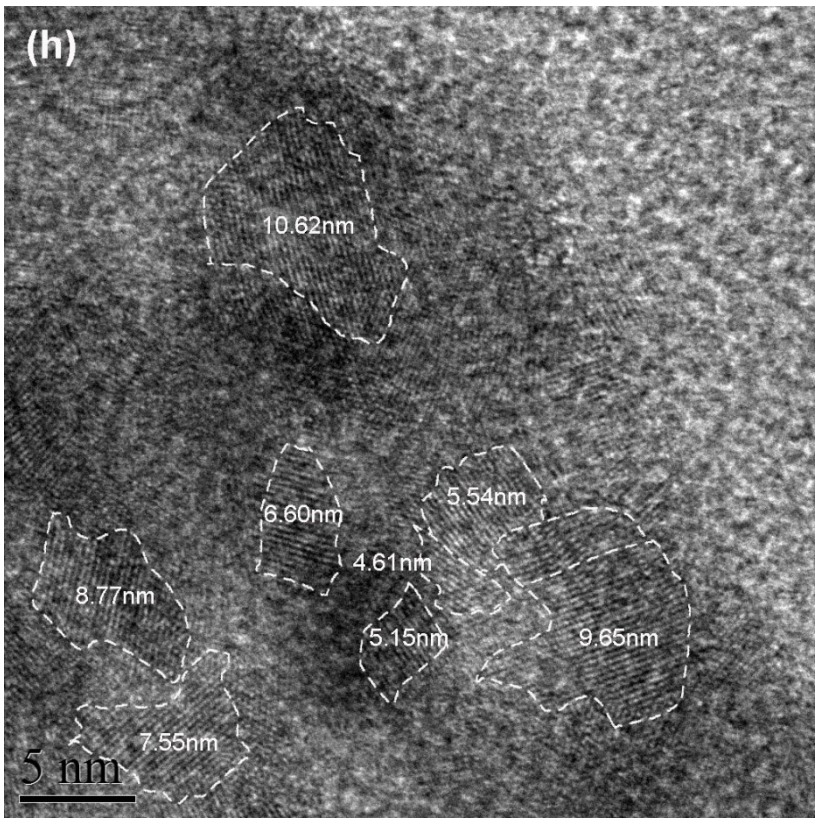
(h)
10.62nm
6.60nm
5.54nm
4.61nm
8.77nm
5.15nm
9.65nm
7.55nm
5 nm

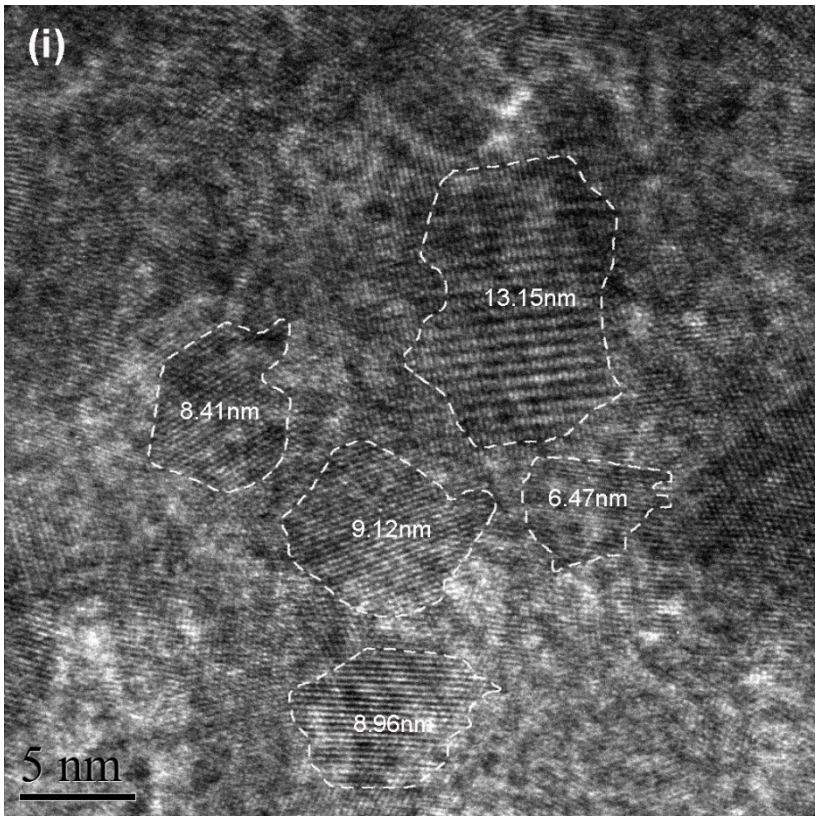
(i)
13.15nm
8.41nm
6.47nm
9.12nm
8.96nm
5 nm

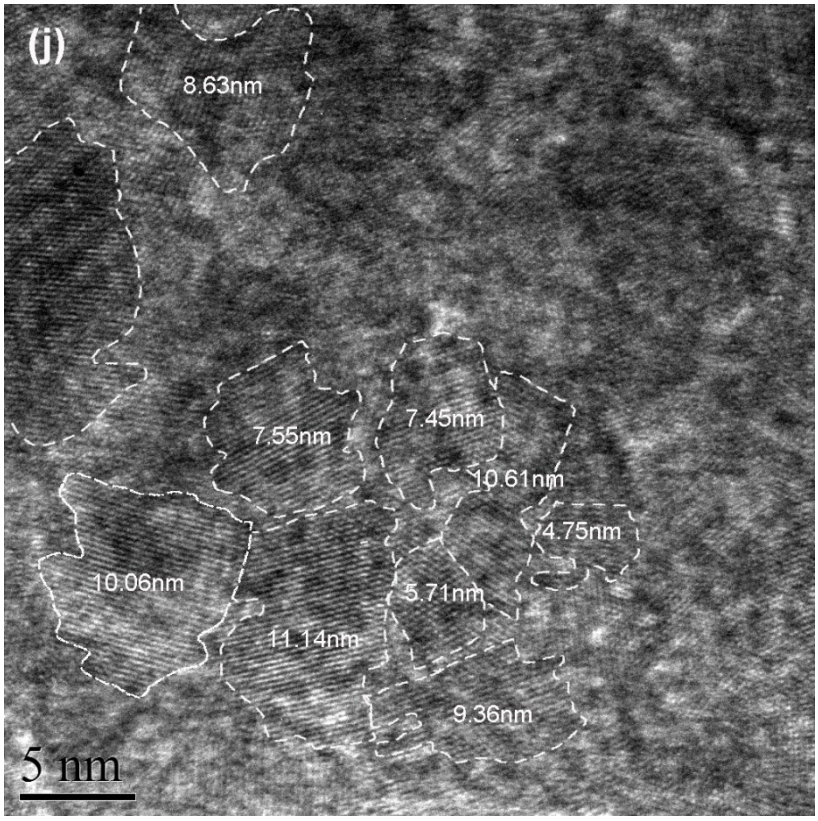
(j)
8.63nm
7.55nm
7.45nm
10.61nm
4.75nm
10.06nm
5.71nm
11.14nm
9.36nm
5 nm

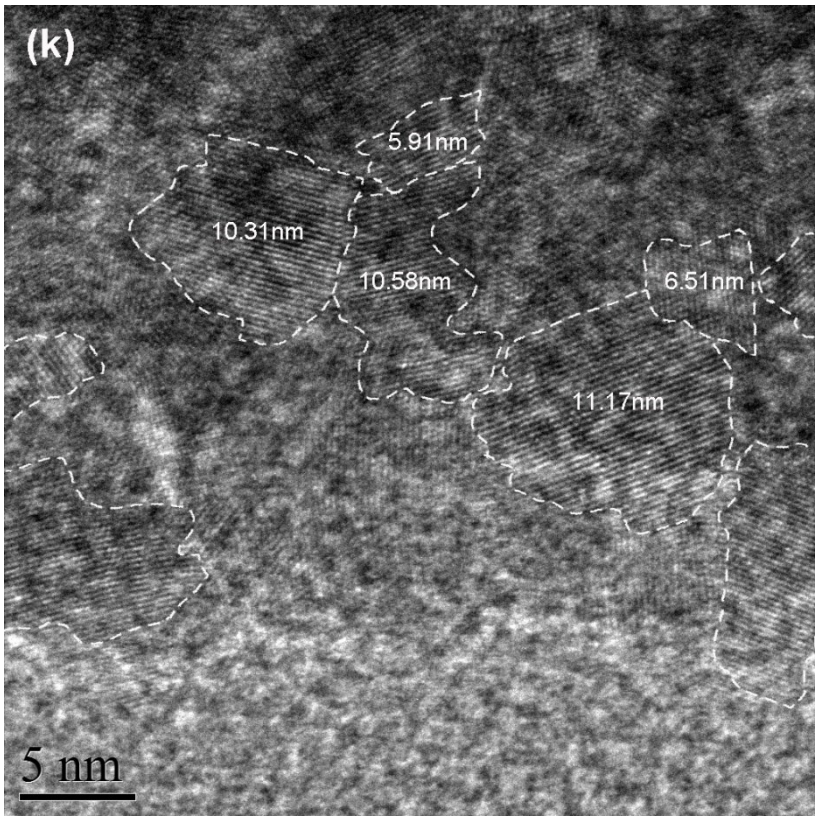
(k)
5.91nm
10.31nm
10.58nm
6.51nm
11.17nm
5 nm

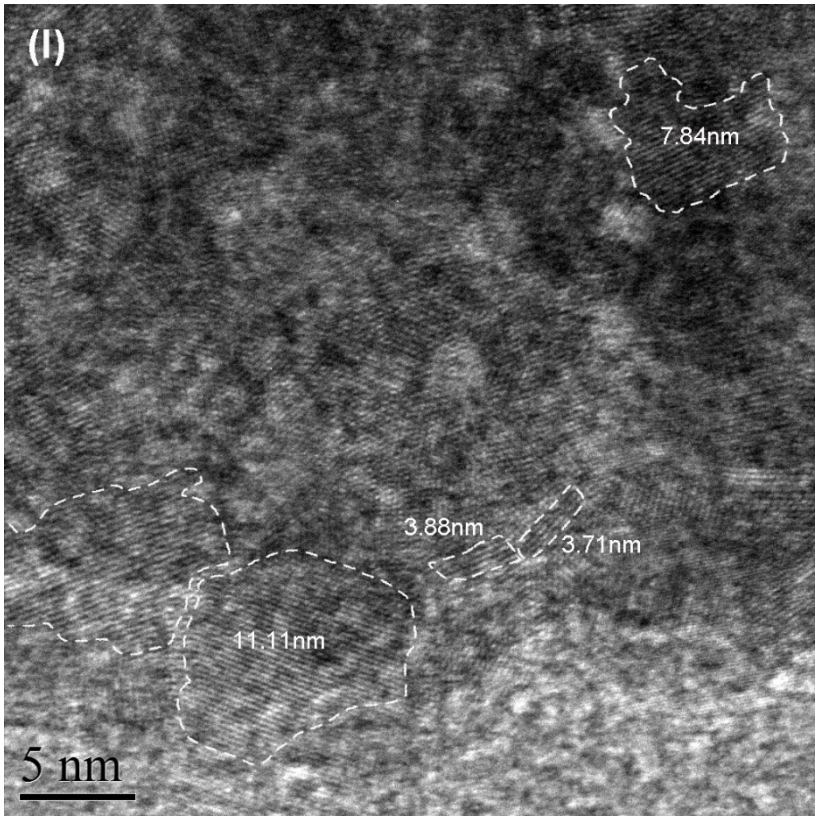
(l)
7.84nm
3.88nm
3.71nm
11.11nm
5 nm

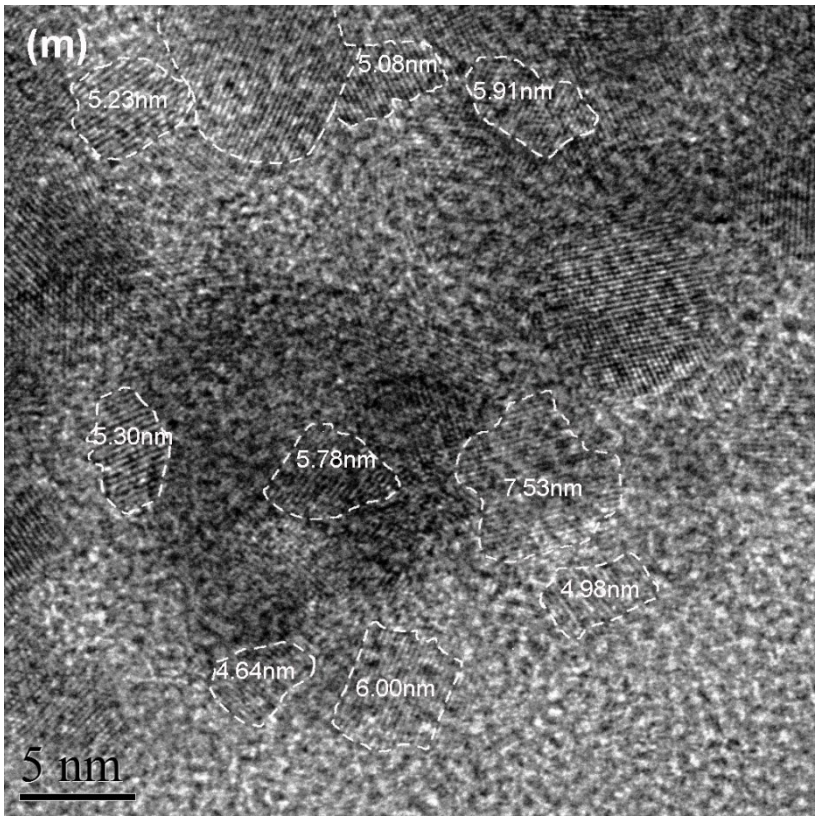
(m)
5.23nm
5.08nm
5.91nm
5.30nm
5.78nm
7.53nm
4.98nm
4.64nm
6.00nm
5 nm

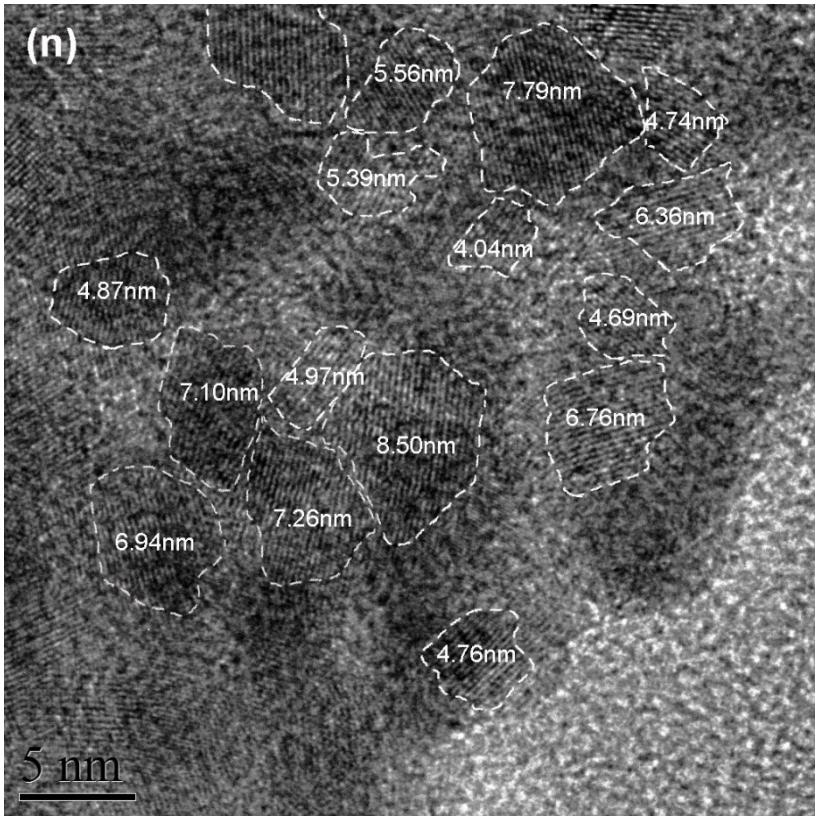
(n)
5.56nm
7.79nm
4.74nm
5.39nm
6.36nm
4.04nm
4.87nm
4.69nm
7.10nm
4.97nm
6.76nm
8.50nm
7.26nm
6.94nm
4.76nm
5 nm

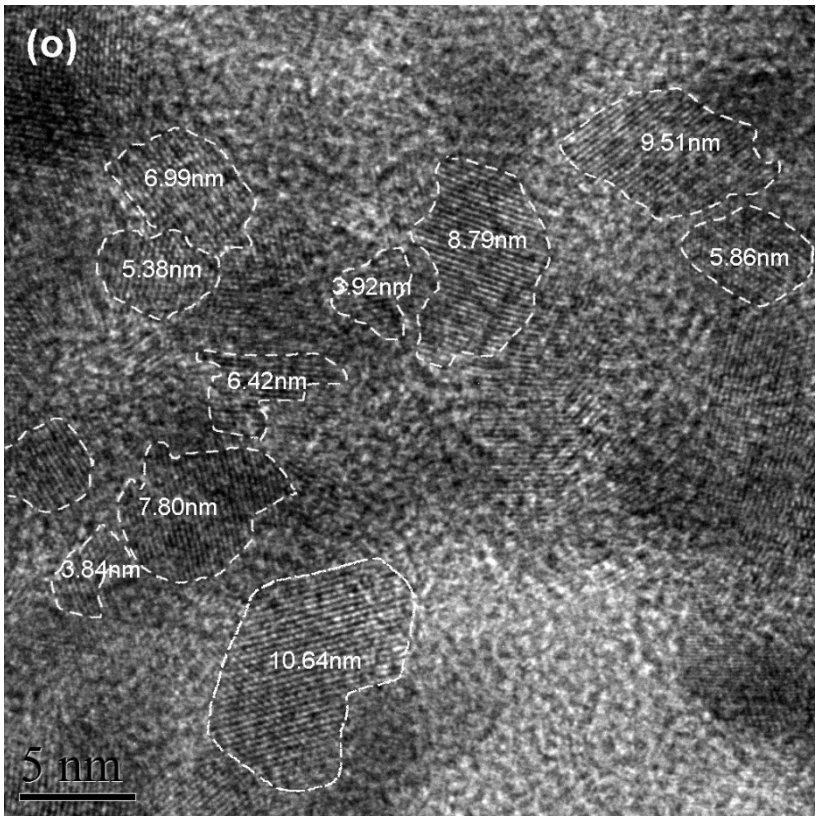
(o)
6.99nm
9.51nm
8.79nm
5.38nm
5.86nm
3.92nm
6.42nm
7.80nm
3.84nm
10.64nm
5 nm

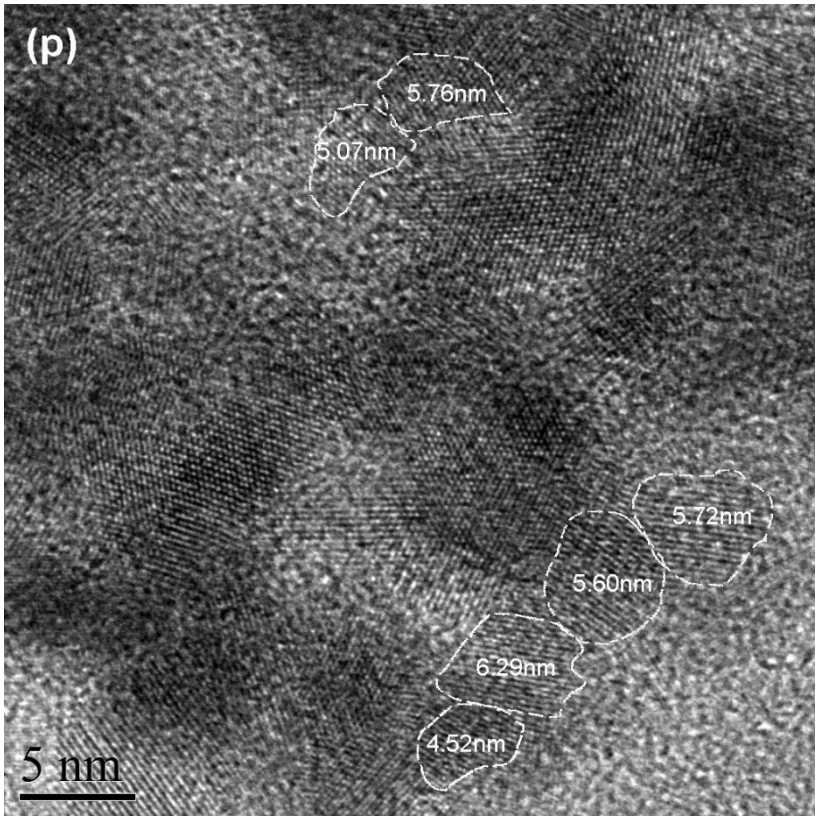
(p)
5.76nm
5.07nm
5.72nm
5.60nm
6.29nm
4.52nm
5 nm

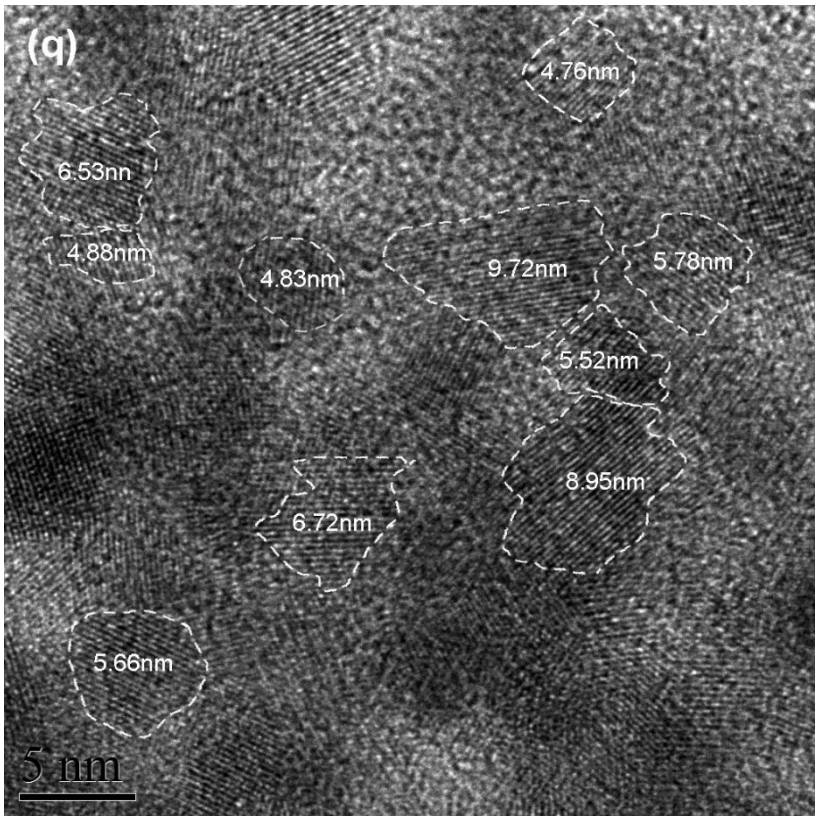
(q)
4.76nm
6.53nn
4.88nm
4.83nm
9.72nm
5.78nm
5.52nm
8.95nm
6.72nm
5.66nm
5 nm

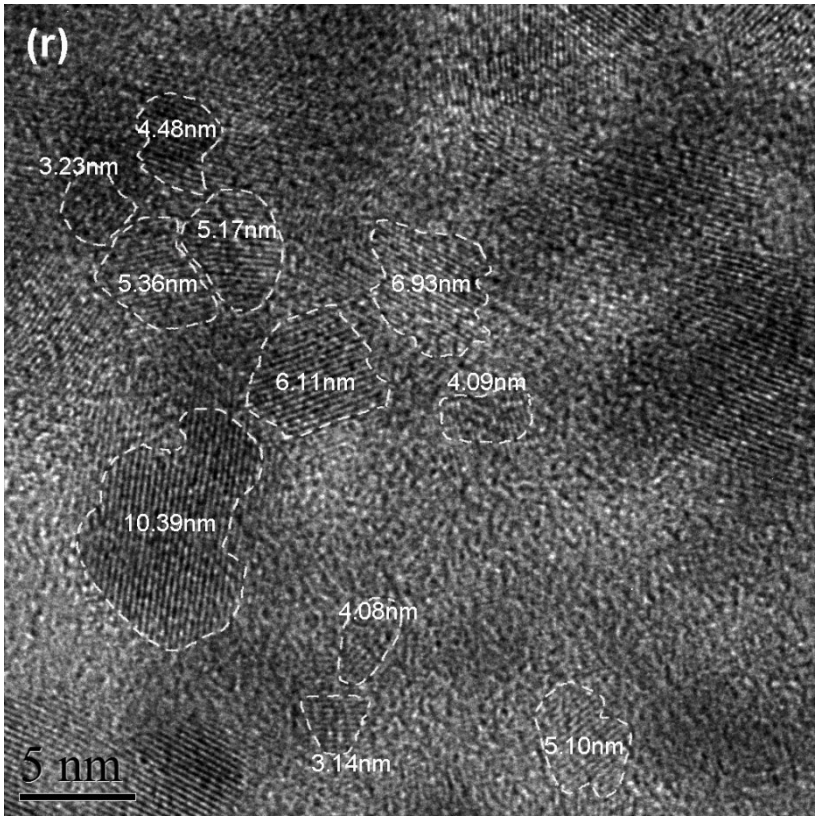
(r)
4.48nm
3.23nm
5.17nm
5.36nm
6.93nm
6.11nm
4.09nm
10.39nm
4.08nm
3.14nm
5.10nm
5 nm

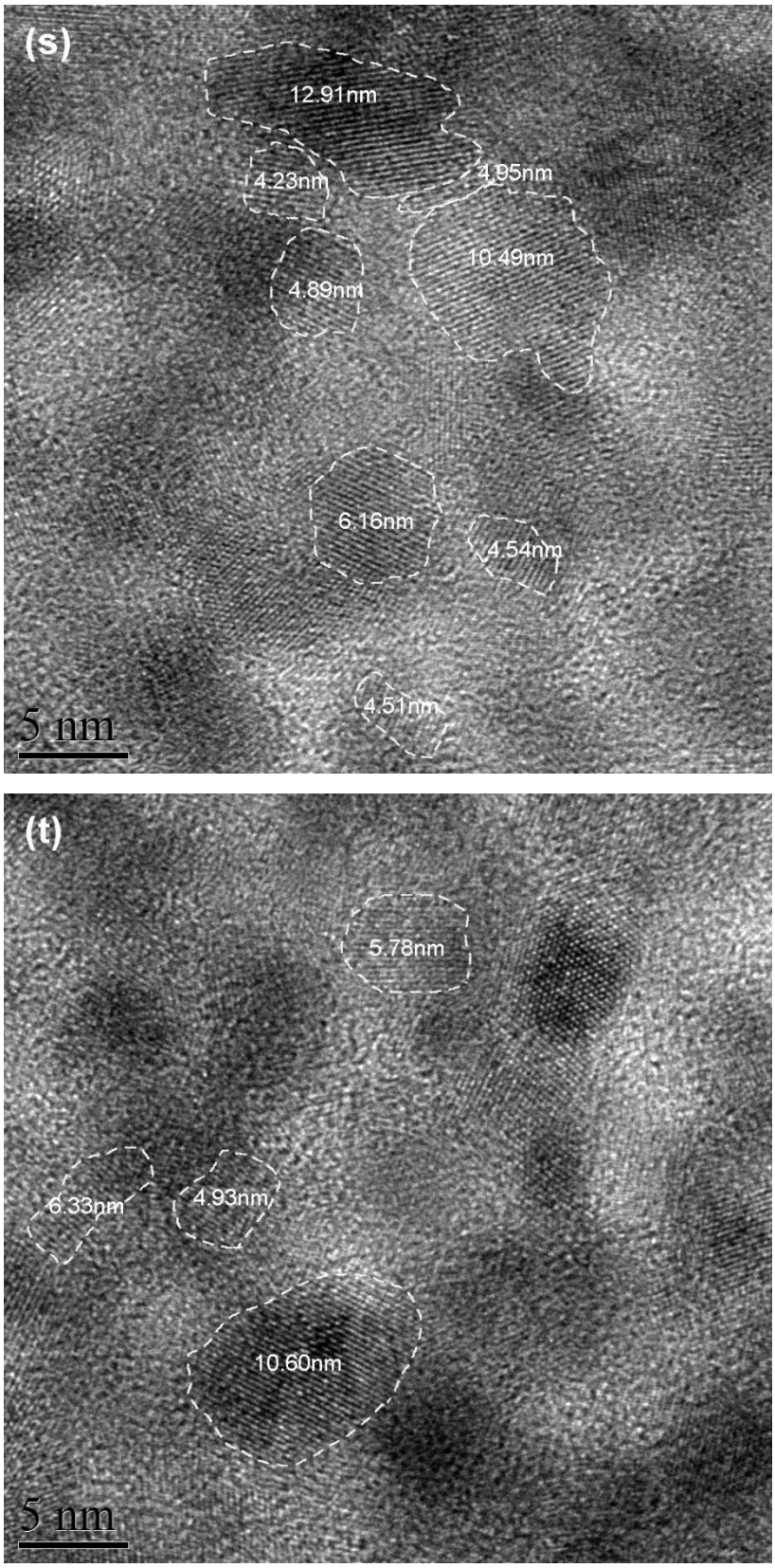

Fig. S1 High-resolution transmission electron microscope images of (a-c) sg-ZnO, (d-l) ic-ZnO and (m-t) as-ZnO films.

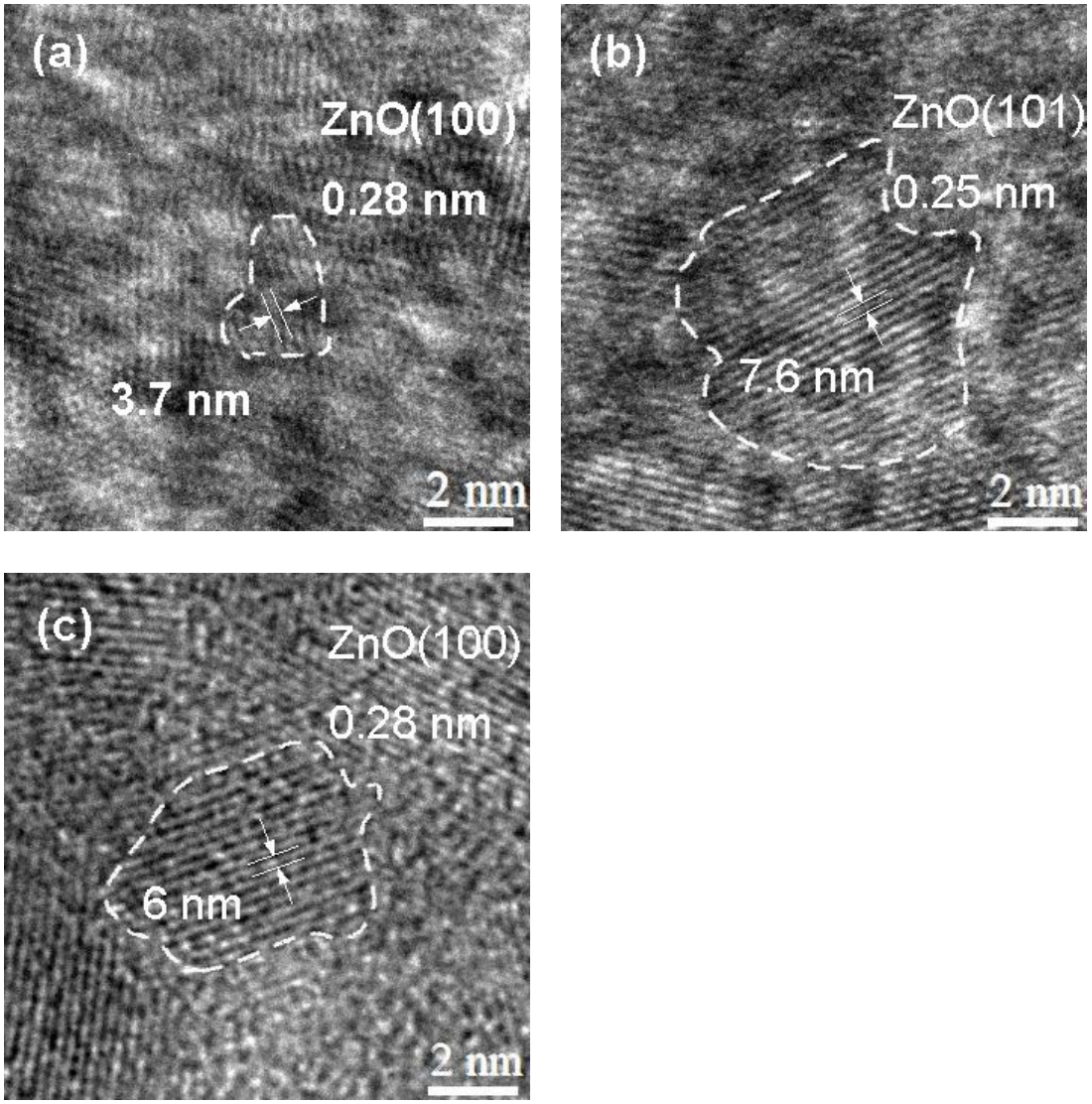

Fig. S2 Representative high-resolution transmission electron microscope images of (a) sg-ZnO, (b) ic-ZnO and (c) as-ZnO.

Table S1 The statistical results of particle size from TEM photos.

Interlayer	Min/nm	Max/nm	Median/nm	Average/nm
sg-ZnO	1.36	8.82	3.32	3.67
ic-ZnO	3.13	15.88	7.49	7.60
as-ZnO	3.14	12.91	5.56	6.08

3. Structural and optoelectronic properties of ZnO films

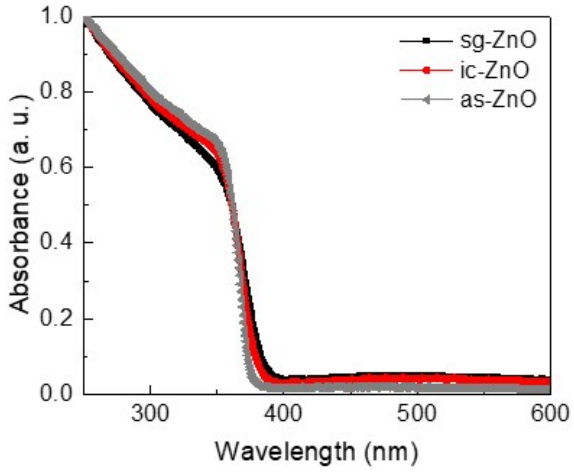

Fig. S3 Normalized UV-vis absorption spectra of neat sg-ZnO, ic-ZnO and as-ZnO films.

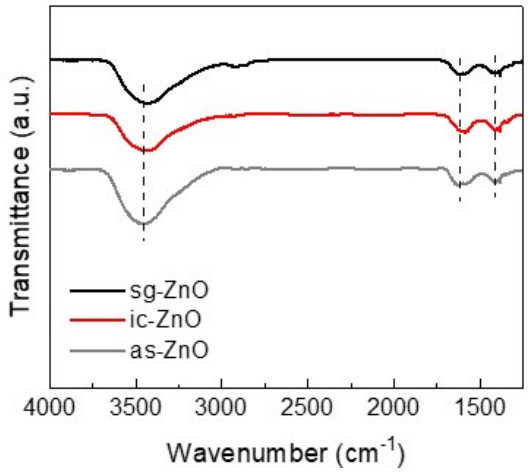

Fig. S4 Fourier transform infrared spectra of sg-ZnO, ic-ZnO and as-ZnO films deposited on KBr substrates.

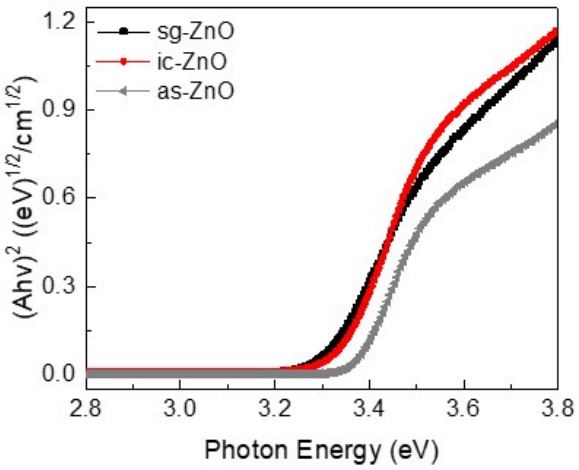

Fig. S5 The bandgaps for sg-ZnO, ic-ZnO and as-ZnO films tested by Tauc plot method.

Table S2 Work function tested by ultraviolet photoelectron spectroscopy.

Interlayer	WF/eV	Bandgap/eV	E_F-VBM/eV	CBM/eV
ITO	4.51	-	-	-
sg-ZnO	3.97	3.29	3.60	-4.28
ic-ZnO	3.98	3.33	3.62	-4.27
as-ZnO	3.89	3.36	3.65	-4.18

Table S3 Electron mobility of various ZnO films tested by SCLC model.

Interlayer	Blend Ratio	Electron mobility/cm^2 V^{-1} s^{-1}
sg-ZnO	-	6.42×10^{-4}
ic-ZnO	1:9	2.39×10^{-3}
ic-ZnO	2:8	2.68×10^{-3}
ic-ZnO	3:7	2.88×10^{-3}
ic-ZnO	4:6	2.50×10^{-3}
as-ZnO	-	1.53×10^{-3}

4. Water contact angle images

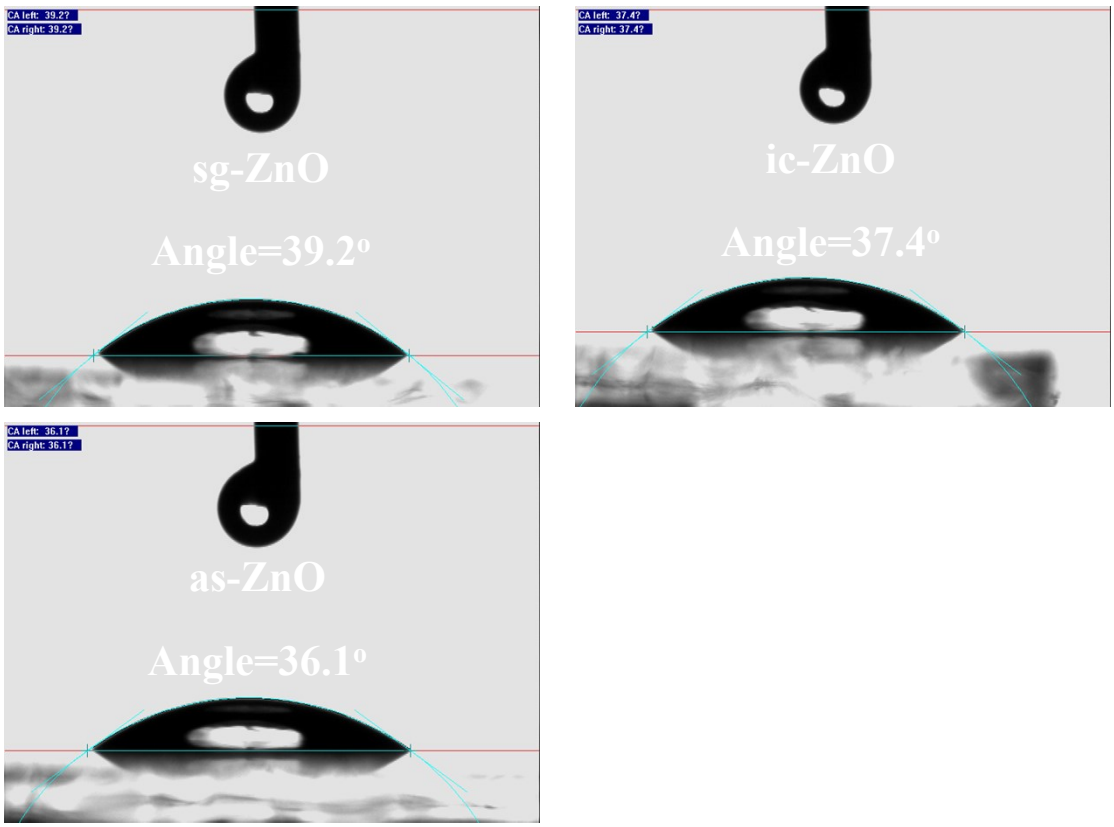

Fig. S6 Water contact angle for ITO/Interlayer(30nm).

5. Device performance

Table S4 Photovoltaic performance of devices based on sg-ZnO, ic-ZnO and as-ZnO using an inverted device structure of ITO/ETL/Active Layer/MoO_3/Al.

ETL	Active Layer	V_{oc} [V]	J_{sc} [mA/cm^2]	FF [%]	PCE (ave.)[a] [%]
sg-ZnO	PTB7-Th:$PC_{71}BM$	0.779	16.68	70.06	9.11(9.06±0.06)
ic-ZnO	PTB7-Th:$PC_{71}BM$	0.779	17.61	70.79	9.72(9.63±0.07)
as-ZnO	PTB7-Th:$PC_{71}BM$	0.779	15.42	69.84	8.40(8.31±0.09)
sg-ZnO	PM6:Y6	0.832	25.45	74.20	15.72(15.34±0.22)
ic-ZnO	PM6:Y6	0.832	26.54	75.20	16.62(16.14±0.27)
as-ZnO	PM6:Y6	0.823	24.71	73.64	14.98(14.71±0.18)

[a] Average PCEs in brackets are based on 10 independent devices.

6. References

1 D. Liu and T. L. Kelly, *Nat. Photonics*, 2014, **8**, 133-138.

2 W. J. E. Beek, M. M. Wienk, M. Kemerink, X. Yang and R. A. J. Janssen, *J. Phys. Chem. B*, 2005, **109**, 9505-9516.